Computers and Electronics in Agriculture 241 (2026) 111303

Contents lists available at ScienceDirect

Computers and Electronics in Agriculture

journal homepage: www.elsevier.com/locate/compag

A novel electrostatic-assisted airflow pollination end-effector for kiwifruit flowers with optimized charging and spraying parameters

Yusong Ding [a,1], Leilei He [a,1], Juncai Huang [a], Xin Wei [a], Yufei Shi [a], Hin Lim [d], Spyros Fountas [e], Shaojin Wang [a,*], Rui Li [a,*], Longsheng Fu [a,b,c,*]

[a] College of Mechanical and Electronic Engineering, Northwest A&F University, Yangling, Shaanxi 712100, China
[b] School of Electronic Information and Artificial Intelligence, West Anhui University, Lu'an, Anhui 237012, China
[c] Jiangxi Provincial Key Laboratory of Modern Agricultural Equipment, Ji'an, Jiangxi 343009, China
[d] School of Engineering, University of Waikato, Hamilton 3240, New Zealand
[e] Agricultural University of Athens, Athens 11855, Greece

ARTICLE INFO

Keywords:
Kiwifruit
Pollination
Electrostatic
End-effector
Induction charging

ABSTRACT

Kiwifruit is a dioecious crop that relies on effective artificial pollination to achieve high yield and superior fruit quality in commercial orchards. Conventional artificial pollination techniques suffer from inherent limitations, as dry powder dispersion leads to substantial pollen loss and liquid spraying causes a rapid decline in pollen viability, collectively resulting in inefficient pollen utilization and inconsistent pollination. To address these constraints, a novel precision end-effector was proposed for electrostatic pollination, which integrated an airflow-assisted delivery mechanism with an electrostatic charging system, enabling directional transport of dry pollen and enhancing its adhesion to flower stigmas. To maximize pollination, the structural design and key operation parameters of the end-effector were optimized to match the unique floral morphology of kiwifruit. The impact of charging parameters, pollination distance, and nozzle size on pollen particle deposition characteristics and rechargeability were evaluated through laboratory experiments. The optimal configuration was determined as induction charging at 18 kV with a 150 mm electrode, and a pollination distance of 5 cm using an 8 mm nozzle. Field experiments conducted in a commercial orchard to verify the effectiveness of the end-effector, achieved a fruit set rate of 96 %. Compared with non-electrostatic pollination, the proposed approach increased average fruit weight by 14.77 %, transverse diameter by 4.16 %, longitudinal diameter by 9.40 %, and seed count by 11.61 %. These results highlight the practical viability of electrostatic pollination in improving pollen utilization and fruit quality for kiwifruit production, offering a promising approach for precision orchard management.

1. Introduction

Pollination is a critical process in kiwifruit production, directly influencing fruit set, size, shape, and quality. As a dioecious crop, kiwifruit requires cross-pollination between male and female plants to achieve successful fruit development (Li et al., 2022b; Broussard et al., 2021). However, natural pollination is often constrained by several factors, including low pollinator activity, adverse weather conditions, and asynchronous flowering between male and female plants (Gudowska et al., 2024; Siviter et al., 2021). As a supplement to natural pollination, artificial pollination has become an essential practice in commercial kiwifruit orchards, which improves fertilization success and contribute to more uniform and marketable fruit (Hao et al., 2025; Abbate et al., 2023; Khatawkar et al., 2021). Despite these advantages, the rising shortage and cost of agricultural labor reduce the practicality and sustainability of manual operations. Especially in large-scale orchards, where flowers must be pollinated with consistent quality within a short pollination window to ensure marketable fruit set rates. Therefore, there is an increasing need for mechanical pollination technology that can improve pollination accuracy, reduce labor dependence, and support standardized orchard management (Li et al., 2022a; Tacconi et al., 2016).

* Corresponding authors at: College of Mechanical and Electronic Engineering, Northwest A&F University, Yangling, Shaanxi 712100, China.
E-mail addresses: shaojinwang@nwafu.edu.cn (S. Wang), ruili1216@nwafu.edu.cn (R. Li), fulsh@nwafu.edu.cn (L. Fu).
[1] The first two authors are co-first authors of the article.

https://doi.org/10.1016/j.compag.2025.111303
Received 18 August 2025; Received in revised form 19 November 2025; Accepted 3 December 2025
Available online 13 December 2025
0168-1699/© 2025 Elsevier B.V. All rights are reserved, including those for text and data mining, AI training, and similar technologies.

According to different pollen application approaches, mechanized pollination of kiwifruit can be divided into dry pollen transfer and wet pollen transfer. Wu et al. (2022) introduced a mobile kiwifruit liquid spray pollinator designed for large-scale orchard pollination, achieving an efficiency of 0.75 mu/h. Tacconi et al. (2016) employed blower-type dry powder dispensers using both pure pollen and pollen-lycopodium mixtures to pollinate kiwifruit, but these approaches resulted in considerable pollen waste by widespread dispersion. Gao et al. (2023) developed a targeted pollination robot equipped with a dual-flow single nozzle, which directly pollinated flowers and effectively reduced pollen loss. However, liquid spraying results in a rapid loss of pollen viability of suspended pollen, limiting its effective pollination window compared with dry pollen (He et al., 2025; Sun et al., 2025). Furthermore, Castro et al. (2021) demonstrated that dry pollen produced a higher proportion of high-quality kiwifruit than wet pollen. Nevertheless, due to its low mass and small size, particles of dry pollen are easily influenced by airflow during dispersion, making it difficult to accurately deposit them on the pistil. This leads to a certain degree of pollen waste and ultimately reduces the economic efficiency of orchard operations.

Electrostatic pollination technology has been proven in several crops to enhance pollen adhesion to pistils while maintaining its viability (Dhalin et al., 2020). The role of electrostatic force was first identified in bee pollination studies, and subsequent measurements confirmed its importance in natural pollination (Clarke et al., 2017; Vaknin et al., 2000). Bechar et al. (1999) simulated the electric field distribution in a charged pollen cloud system near grounded flowers and analyzed the trajectories of pollen particles, which showed that electrostatic pollination doubled the yield of dates by field experiments. Vaknin et al. (2001) reported that charged pollen was more likely to settle on pistils than petals, which improves utilization efficiency. Despite these promising biological findings, the application of electrostatic principles in practical agricultural devices remain technically challenging, particularly in achieving controlled pollen deposition and charge regulation. Gan et al. (2003) developed an electrostatic pollinator for almond, kiwifruit, and date, which showed that applying electrostatic charge to pollen can effectively reduce pollen drift while increasing yield. While electrostatic pollination has proven effective in enhancing pollen adhesion and yield across various crops, most existing systems still rely on wide-area spraying with limited control over pollen trajectory and charging parameters.

Selecting appropriate pollen charging parameters can enhance effective pollen deposition and reduce pollen loss. Patel et al. (2017) developed an electrostatic nozzle for pesticide spraying, achieving a charge-to-mass ratio exceeding 10 mC/kg at voltages below 2.5 kV, which increased droplet deposition by two to three times compared with uncharged spraying. Bechar et al. (2008) showed that aligning a charged ring electrode with the edge of the main electrode improved pollen deposition to tree models by 76 % compared with positioning it 40 mm behind. Mohanty et al. (2024) used response surface methodology to optimize voltage, electrode diameter, and spray distance in an electrostatic liquid spraying system, achieving 1.5 to 4.6 times greater droplet deposition than in uncharged spraying. While established researches provide valuable insights into electrostatic spraying, most of them focus on general spraying systems rather than pollination end-effectors for specific crops (Zhang et al., 2021). Given the unique floral morphology of kiwifruit, further research is needed to develop crop-specific configurations and structural adaptations for efficient, targeted pollen delivery. To address these challenges, this study develops an electrostatic-assisted airflow pollination end-effector that integrates airflow-guided delivery with induction charging, enabling precise, controllable, and crop-specific pollen deposition for kiwifruit flowers.

This study proposed an end-effector based on electrostatic technology for precision pollination of kiwifruit, and systematically investigates its effectiveness through controlled experiments and field verification. To inform its configuration, a statistical analysis of flower morphological parameters was conducted, followed by experiments examining the effects of varying pipe diameters and pollination distances on pollen coverage. These experiments enabled the identification of the optimal pipe size and effective working range for field operations. Additionally, the influence of key charging parameters, including charging voltage, method of charge generation, and electrostatic ring diameter on the charge-to-mass ratio of pollen was explored to optimize the charging system. Finally, the performance of the electrostatic pollination method was evaluated against non-electrostatic pollination through comparative field experiments.

2. Materials and methods

2.1. Pollination agronomic analysis of kiwifruit

The development of an end-effector for kiwifruit pollination should be guided by its agronomic traits, particularly the spatial distribution of flowers and specific environmental requirements necessary for effective pollination. In standardized orchards, kiwifruit is typically cultivated on trellis systems, with flowers concentrated beneath the canopy at a height of approximately 180 cm, as shown in Fig. 1a. These flowers tend to grow in clusters and orient downward, which favors bottom-up pollen delivery by artificial pollination, as shown in Fig. 1b. Due to the short and synchronized flowering period, the optimal window for pollination is limited to the first three days after petals unfold. This constraint necessitates the development of end-effectors that combine high operational efficiency with structural simplicity to meet the demands of timely, high-intensity operations.

Environmental conditions, particularly air humidity, play a crucial role in determining the effectiveness of flower pollination. The ideal relative humidity for kiwifruit pollination ranges from 60 % to 80 %, both excessively high and low humidity can negatively impact pollen viability and reduce pollination efficiency. Shaanxi Province in China, a major kiwifruit planting area in the world and the field experiment site for this study, typically experiences relatively low humidity of about 45 % to 65 % during the pollination season each year, which affects the adhesion of dry powder particles and the overall pollination efficiency. However, in low-humidity environments, the reduced moisture content in the air increases the electrical insulation between pollen particles and the surrounding air, leading to stronger electrostatic accumulation that benefits electrostatic pollination operations.

2.2. Composition of the developed end-effector

Electrostatic pollination technology offers a promising approach to improving fertilization efficiency by utilizing the attractive force between electrically charged pollen particles and the flower pistils. The developed end-effector consists of two functional subsystems, an airflow supply system, and a charging system. The charging system imparts unipolar electric charges to pollen particles, allowing them to be electrostatically attracted to the floral pistils. While the airflow supply system was designed to generate a stable, directed stream that could transport the charged pollen as a fine aerosol toward the flowers. The coordinated operation of these two subsystems enables controlled, uniform, and efficient pollen delivery under field conditions.

Structurally, the end-effector integrates pollen mixing, charging, and transport into a compact assembly. During operation, air generated by an air pump enters the pollen storge tank through an inlet hose equipped with a high-pressure nozzle to refine and accelerate the stream. Inside the tank, pollen is mixed with the air to form a uniform suspension, which exits through an outlet. As the pollen travels along the pipe, it passes through a charging zone where it acquires an electrostatic charge. The charged pollen particles are then directed toward the flower pistils, under the influence of electrostatic forces. Composition of the developed end-effector is shown in Fig. 2, and additional technical specifications and operational details are provided in the following sections.



Fig. 1. Standard cultivation mode of kiwifruit with trellis structure (a) and downward flower orientation (b).

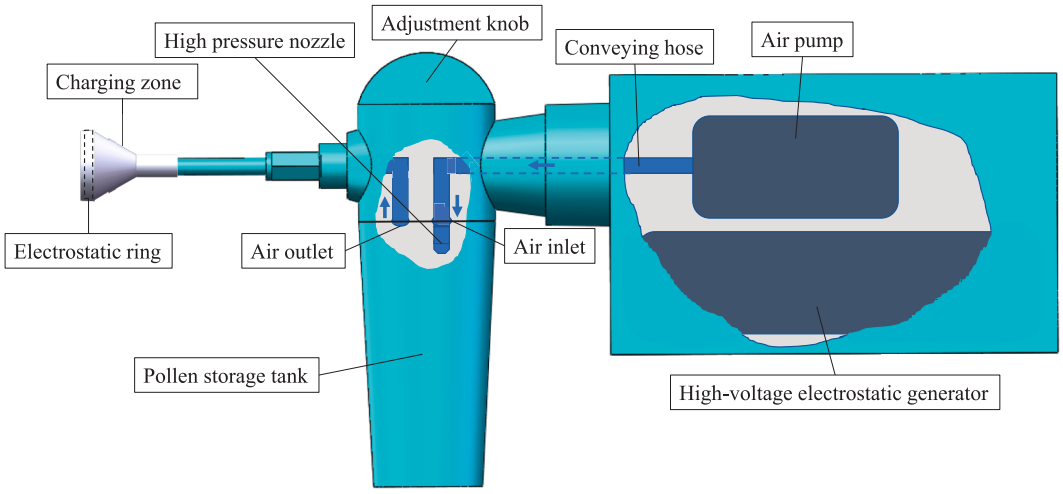


Fig. 2. Structural composition of the designed electrostatic pollination end-effector.

2.3. Airflow supply system

The airflow supply system primarily comprises of an air pump and a pollen storage tank. Air from the pump acts as the driving force for pollen transport within the end-effector and for directional dry powder dispersion outside. Due to the extremely light nature of kiwifruit pollen particles (with approximately 2.79×10^5 particles contained in just 1 mg of pure pollen) even minimal airflow under natural conditions can easily disperse them. Therefore, effective directional pollination requires an airflow strong enough to carry pollen particles to the pistils for successful deposition. To balance portability, reliability, and energy efficiency under field conditions, a compact cylindrical pump was selected, featuring a 6 cm base diameter, 11 cm height, 12 W rated power, and 15 L/min flow rate. This configuration ensures adequate airflow for pollen transport while minimizing power consumption and mechanical disturbance to floral structures.

2.4. Charging system

2.4.1. Charging system design

Dry pollen particles can be charged by either ionization or induction. In ionization charging, a high-voltage direct current is applied to a sharp electrode, creating a corona discharge that ionizes the surrounding air (Ou et al., 2025). The resulting ionized field allows free ions to attach to dispersed particles as they pass through, thereby imparting a net electric charge. In induction charging, a high-voltage potential is applied to a ring electrode placed near the pipe outlet, generating a strong electric field that enables pollen particles to acquire an induced charge without directly contacting the electrode (Mamidi et al., 2013). Both methods are powered by a high-voltage electrostatic generator with a power consumption of 1.2 W and an adjustable output voltage range of 0 to 30 kV. During the development of the end-effector, both methods were tested and the performances were evaluated. An electrostatic ring was integrated with the pipe outlet, enabling pollen particles to acquire charges as they travel through the field, thereby enhancing their deposition efficiency on floral pistils, as shown in Fig. 3.

2.4.2. Experiments on pollen charge-to-mass ratio

Electrostatic adhesion of pollen is the process by which charged pollen particles are propelled and deposited onto the pistil of kiwifruit flowers under the combined influence of electrostatic force, gravity, and

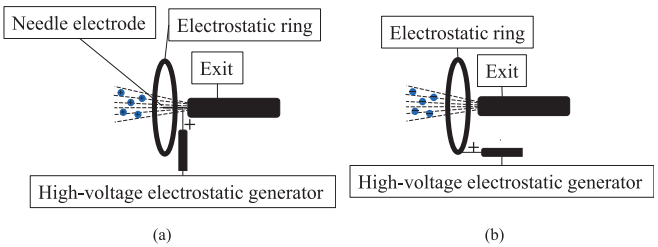


Fig. 3. Schematic diagram of ionization charging (a) and induction charging (b).

airflow resistance. The equation governing pollen motion is shown by Eq. (1), as introduced by Bechar et al. (2008):

$$F_p = EQ_p - mg - \frac{1}{2}\rho v^2 C_d A \quad (1)$$

The upward vertical direction is considered as the positive direction, where F_p refers to resultant force exerted on the pollen particle; E refers to electric field; Q_P refers to pollen electric charge; m refers to mass of the pollen; g refers to gravitational acceleration, 9.81 m/s^2; ρ refers to airflow density; v refers to relative velocity of pollen to airflow; C_d refers to drag coefficient; A refers to cross-section area of the pollen.

A theoretical analysis was developed to evaluate electrostatic, gravitational, and aerodynamic forces acting near the nozzle outlet. It was assumed that pollen particles acquire uniform unipolar charges after passing through the induction charging region, where the local electric field exerts a directional force guiding them toward the target surface. By comparing the relative strengths of these forces, the analysis identifies the threshold conditions under which electrostatic attraction governs particle motion. These thresholds were used to guide the optimization of operational parameters, including applied voltage, electrode geometry, and pollination distance, ensuring that pollen deposition occurs efficiently and directionally.

During the pollination process, electrostatic forces facilitate pollen deposition by attracting charged particles toward the pistil, while gravity acts in the opposite direction. Since both the pollen particles and the air exit the pipe with the same initial velocity, and drag from the airflow maintains their relative velocity near zero, airflow resistance is neglected in the analysis. To enhance electrostatic adhesion, it is necessary to maximize the electrostatic force acting on the particles while minimizing the opposing effect of gravity. As such, the charge-to-mass ratio becomes a critical parameter, as a higher ratio increases the influence of electrostatic attraction on pollen movement, thereby improving deposition efficiency and uniformity on the pistil.

To achieve quantitative evaluation, a custom-designed Faraday cylinder equipped with an electrostatic meter was employed to measure the charge-to-mass ratio of kiwifruit pollen. The Faraday cylinder consisted of a dual-cylinder structure made of stainless steel, composed of an inner and an outer cylinder separated by an insulating layer. The inner cylinder measured 16 cm in height and 5.5 cm in diameter, while the outer cylinder measured 18 cm in height and 6 cm in diameter, as shown in Fig. 4. The inner cylinder was responsible for collecting charged pollen particles and transferring their total charge to the electrostatic meter for quantification. Meanwhile, the outer cylinder functioned as an electromagnetic shield, effectively minimizing external interference, and ensuring that only the charge accumulated in the inner cylinder was measured, thereby improving the accuracy of the readings.

The electrometer measured the charge-to-mass ratio of pollen by detecting the deflection of a metal pointer induced by electrostatic forces. It comprises a cylindrical metal casing, a metal rod, a metal pointer, and an insulator. The casing functions both as a protective enclosure for the internal components and as one plate of a capacitor. The metal rod passes through the insulator, with its upper end connected to a metal sphere electrically linked to the inner cylinder of the Faraday cage via a conductive wire, and its lower end supporting a freely rotating horizontal metal pointer. The insulator electrically isolates the rod from the casing, minimizing external interference. When charged pollen enters the inner cylinder of the Faraday cage, the charge is transferred to the cylinder and then conducted to the electrometer, charging the rod and pointer, and inducing opposite charges on the inner surface of the casing. The resulting electric field causes the pointer to deflect, with the deflection angle proportional to the magnitude of the charge. The total charge is determined from the measured deflection angle, and the corresponding pollen mass is obtained from the weight difference of the Faraday cylinder before and after dry powder spraying, enabling calculation of the charge-to-mass ratio.

To evaluate the effects of charging method, charging voltage, and electrostatic ring diameter on the charge characteristics of the end-effector, a series of controlled experiments were conducted. Two charging methods were primarily evaluated based on the charge-to-mass ratio of pollen under varying charging voltages and electrostatic ring diameters. During each experiment, the Faraday cylinder was positioned 5 cm in front of the pipe to collect charged pollen particles. Each dry powder spraying session lasted for 60 s and was precisely controlled by a computer. After dry powder spraying, the deflection angle of the electrostatic meter connected to the Faraday cylinder was recorded to determine the total electric charge of the collected pollen. Meanwhile, the mass of the Faraday cylinder before and after dry powder spraying was measured using a digital balance with a precision of 0.01 g. The mass difference was used to calculate the amount of pollen deposited. To ensure reliability and reduce measurement error, each experiment was repeated three times, and the average values were recorded for subsequent analysis. After each experiment, residual pollen inside the Faraday cylinder was thoroughly cleaned to prevent cross-contamination and maintain consistent experimental conditions.

2.5. Experiment on pollen coverage area

To determine the key parameters of the end-effector, ensure

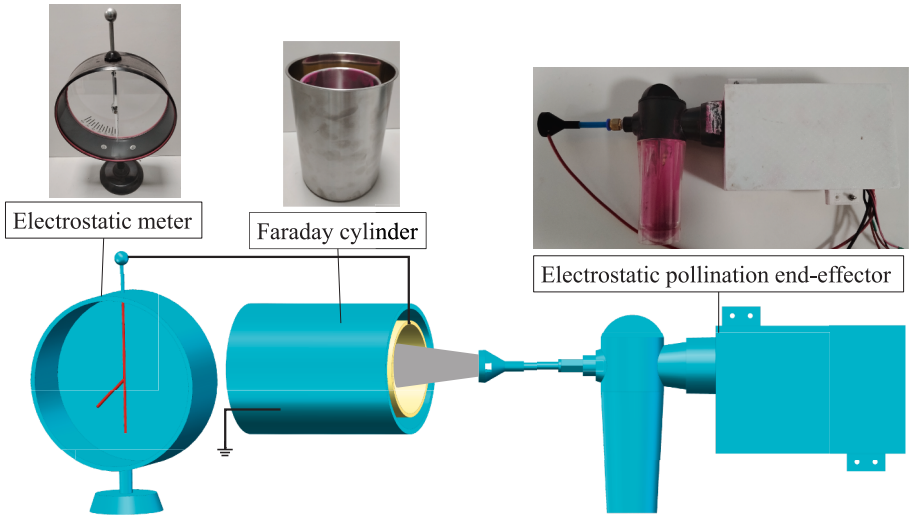


Fig. 4. Experimental system for pollen charge-to-mass ratio measurement with dual-cylinder Faraday cage and electrostatic electrometer.

maximum coverage of the pistil region, and minimize coverage of non-pistil areas, the physical dimensions of kiwifruit flowers were measured and analyzed. A total of 1,255 individual kiwifruit flowers were manually measured using vernier calipers and measuring tape (Gao et al., 2025). Data collection was conducted at the International Kiwifruit Innovation Orchard in Yangling, Shaanxi, China (34°17′N, 108°2′E, approximately 504 m in altitude). The results showed that the mean overall flower diameter was 55.3 mm, with a standard deviation of σf = 9.8 mm (shown in Fig. 5b). The mean diameter of the pistil region was 24.3 mm, with a standard deviation of σp = 12.4 mm (shown in Fig. 5c). To maximize pollen deposition on the pistil rather than on non-reproductive floral structures such as petals, the dry powder spray coverage should ideally be as close as possible to the lower bound of 24.3 mm.

Pollination distance and outlet pipe diameter jointly determine the dispersion and coverage range of the pollen, both of which are critical parameters for effective kiwifruit pollination. To determine the optimal values of these two parameters, experiments were conducted under non-electrostatic conditions using outlet pipes with diameters of 4 mm, 6 mm, 8 mm, 10 mm, and 12 mm at various distances to evaluate the spatial coverage of the pollen mixture. The pollen mixture was prepared at a 1: 2 ratio of kiwifruit pollen to dyed Lycopodium spores, consistent with field operational standards, to accurately simulate real pollination conditions. In each experiment, an 11 cm diameter filter paper was placed horizontally above the outlet of the end-effector, at distances ranging from 1 cm to 10 cm. The end-effector was mounted on an adjustable leveling lift table to precisely control the pollination distance. The filter paper was pre-moistened to improve adhesion and capture of the pollen mixture. For each experiment, dry pollen was sprayed for two seconds. After pollen spraying, the stained area on the filter paper was measured in four orthogonal directions using a measuring tape, and the average of the four diameters was recorded as the effective coverage range. Each experiment was repeated three times for each distance and pipe diameter combination, and the average was used to ensure accuracy and consistency (shown in Fig. 6).

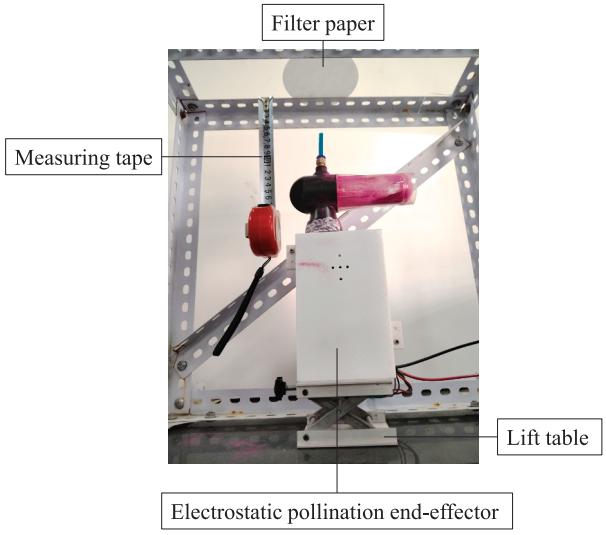


Fig. 6. Experimental platform for evaluating pollination parameters, incorporating an adjustable end-effector mount, interchangeable outlet pipes, and a filter-paper.

2.6. Field experiment on electrostatic pollination of kiwifruit

A field experiment was conducted to evaluate the effectiveness and advantages of electrostatic pollination on kiwifruit. The experiment was carried out at the Yangling International Kiwifruit Innovation Orchard in Yangling, Shaanxi Province, China (34°17′N, 108°2′E, approximately 504 m in altitude). A randomized complete block design was employed, consisting of two treatments that used the same developed end-effector. In the electrostatic-assisted pollination treatment, the charging system was activated, while in the non-electrostatic control, the system remained deactivated. To minimize variability from pollen sources, both treatments used identical pollen mixtures collected from the same batch. Within each block, 80 flowers were selected and evenly divided between the two treatments. Flowers were chosen in matched pairs from the same vine to reduce plant-specific variation, and the pollination sequence within each block was randomized to eliminate positional bias. Each pollination operation was automatically controlled by a computer program, and the spraying duration was standardized at one second per flower. Seven days after pollination, the fruit set rate was recorded. When the fruit matured, 30 kiwifruit samples were randomly harvested from each treatment group for quality evaluation.

3. Results and discussion

3.1. Experimental evaluation of pollen charge-to-weight ratio

The charge-to-mass ratio of pollen under ionization and induction charging were evaluated at varying voltage levels. For both methods, the charge-to-mass ratio initially increased with voltage and then declined after reaching a peak. For ionization charging with a 20 mm diameter

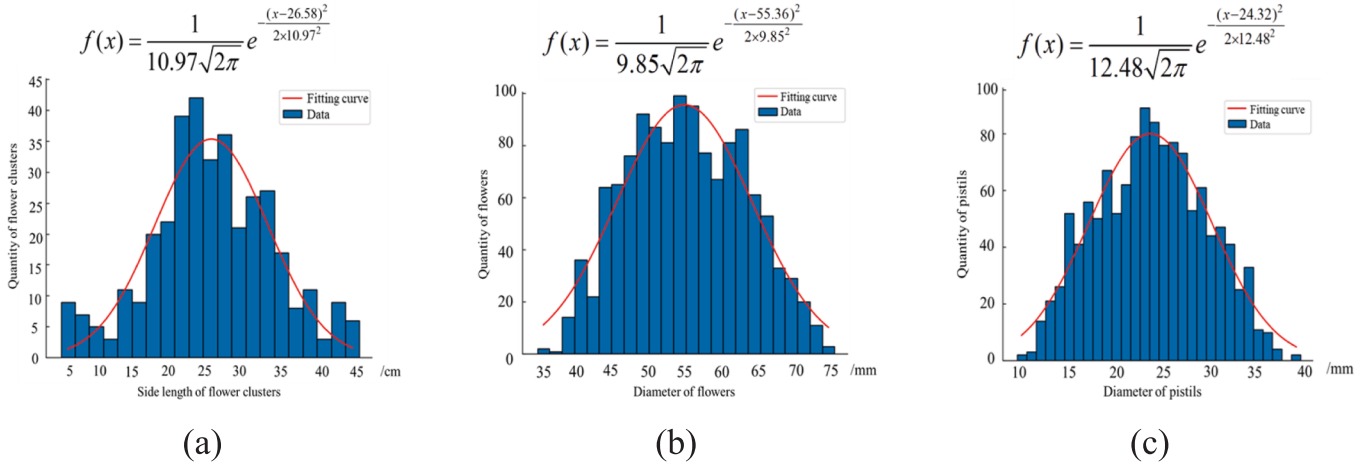


Fig. 5. Distribution of kiwifruit flower dimensions with minimum bounding rectangle side length of flower clusters (a), external circle diameter of flowers (b), and external circle diameter of the pistil area (c).

electrostatic ring, the charge-to-mass ratio increased gradually at lower voltages, but surged sharply once the voltage exceeded 8 kV, reaching a peak of 30.4°/g at 24 kV (shown in Fig. 7). This behavior reflects the threshold effect inherent to ionization, where a sufficiently high voltage is required to initiate substantial corona discharge and enable effective charge transfer to pollen particles.

In contrast, the induction charging exhibited a rapid increase in charge-to-mass ratio at a lower voltage level, with the rate of growth gradually decreasing as voltage increased further. This can be attributed to the enhancement of the electric field at higher voltages, which facilitates charge induction on pollen surfaces (Patel et al., 2017). Beyond a critical voltage threshold, both charging methods exhibited saturation characteristics, as continued increase in voltage degraded the chargeability of pollen particles. Notably, induction charging reached saturation at a lower voltage than ionization charging. It achieved a higher charge-to-mass ratio in the low-voltage range under the same experimental conditions, with a maximum of 29.6°/g at 18 kV. Considering the safety concerns associated with high-voltage electrostatic operation, induction charging was selected as the preferred approach for the end-effector.

The diameter of the ring electrode strongly influenced charging efficiency in induction charging. For a given electrode diameter, the charge-to-mass ratio increased with voltage up to a critical point. When the voltage exceeded approximately 18 kV, partial corona discharge occurred, shifting the mechanism toward ionization charging and thereby reducing the charge-to-mass ratio (Han et al., 2024). Smaller electrode diameters produce stronger electric field intensities, enabling higher charge-to-mass ratio under the same voltage conditions. Results indicated that although the voltage corresponding to the peak charge-to-mass ratio is similar across the three diameters, the 15 mm electrode achieved the maximum charge-to-mass ratio (shown in Fig. 8). This can be attributed to the fact that smaller inner diameters enhance the radial electric field, thereby generating stronger electrostatic forces (Mohanty et al., 2024). These forces improve the uniformity of pollen dispersion and spatial distribution, ultimately leading to higher overall charging efficiency. Therefore, an induction charging configuration with an electrode diameter of 15 mm and a voltage of 18 kV was determined to be optimal, balancing high charging efficiency with operational safety.

3.2. Evaluation of pollen coverage area in experiments

Under the set experimental conditions, the pollen coverage area exhibited a clear increasing trend with both pollination distance and outlet pipe diameter. Detailed experimental data demonstrate that at a fixed pollination distance, larger pipe diameters produced broader pollen coverage diameters. At a distance of 1 cm, the coverage diameter rose from 5.12 mm with a 4 mm pipe to 16.41 mm with a 12 mm pipe. Meanwhile, the corresponding coverage diameters were expanded to 23.51 mm and 33.91 mm, respectively (shown in Fig. 9). This effect is attributed to the wider spray angle of larger outlet diameters, which allows greater airflow volume and produces a broader initial dispersion. Pollen coverage diameter increased with pollination distance but the rate of increase slowed as the distance grew with a noticeably slower increase at longer distances (shown in Fig. 9).

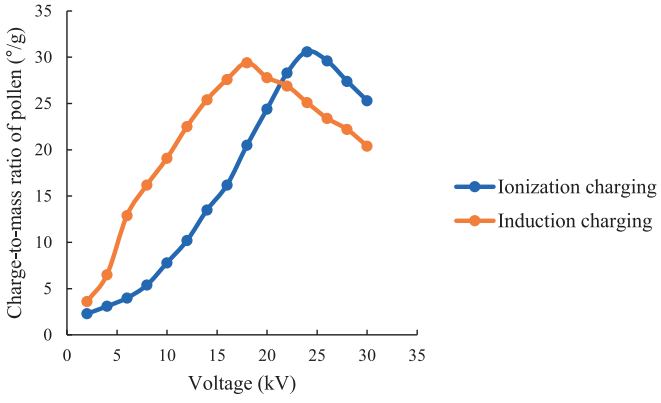


Fig. 7. Effects of charging method and voltage on pollen charge-to-mass ratio.

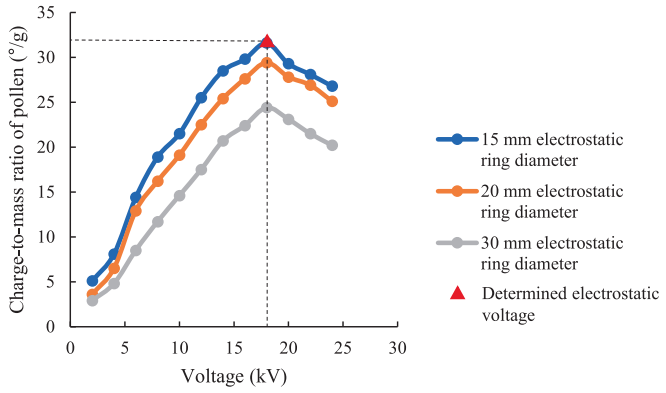


Fig. 8. Influence of induction ring size on pollen charge-to-mass ratio in induction charging.

In general, the pollen coverage diameter increases with the increase in pollination distance, and the coverage change rate gradually decreases. Mechanistically, pollen diffusion after ejection is primarily influenced by pollination distance and airflow velocity. The generated airflow from the constant-flow pump exhibits an inverse relationship between velocity and outlet diameter. Larger diameters enhance initial coverage but lower airflow speed, thus reducing effective pollen delivery to the pistil at longer distances, particularly under variable orchard environmental conditions (Zhao et al., 2008). Excessive pollination distance also exacerbates pollen loss and gradually decreases the charge-to-mass ratio due to prolonged interactions with ambient opposite charges (Patel et al., 2017). Considering floral morphology measurements, the optimal pollen coverage diameter was determined to be approximately but not less than 24.3 mm. Consequently, to achieve an optimal balance between deposition efficiency and pollen conservation, an 8 mm pipe diameter combined with a 5 cm pollination distance was selected, yielding a pollen coverage diameter of approximately 26.21 mm.

3.3. Evaluation of field experiments on kiwifruit electrostatic pollination

Electrostatic pollination outperformed non-electrostatic pollination in both fruit set rate and fruit quality. The fruit set rate reached 96.25 % for the electrostatic treatment compared to 93.75 % for the non-

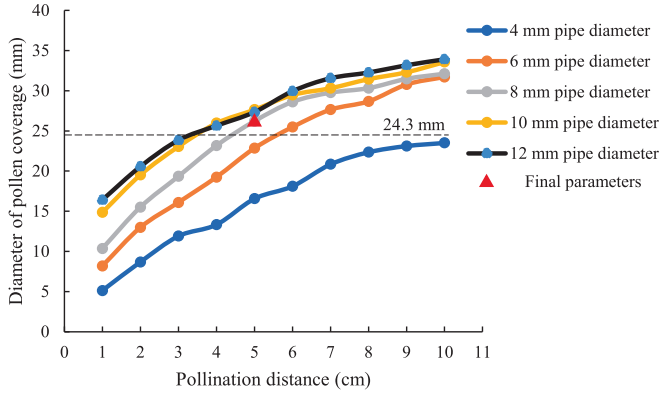


Fig. 9. Effect of pipe diameter and pollination distance on pollen coverage diameter.

electrostatic treatment. For the non-electrostatic pollinated group, the average seed count was 620.33 per kiwifruit. In contrast, the electrostatic pollination group achieved an average seed count of 692.33, reflecting an 11.61 % increase (shown in Table 1). These results demonstrate that electrostatic pollination not only maintained a high fruit set rate but also improved seed formation, indicating better overall pollination effectiveness. Analysis of variance (ANOVA) was employed and confirmed the statistical significance of this improvement ($F = 4.196$, $p = 0.017$), indicating that electrostatic pollination has a positive and significant effect on pollination performance.

The fruit set rate and quality of kiwifruit after pollination are directly related to stigma coverage. While pollination of a single stigma can initiate fruit development, covering more stigmas generally leads to higher fruit weight and seed number, with quality improvements plateauing when coverage reaches approximately 17 stigmas (Nakao et al., 2025). When applying electrostatic pollination, pollen particles carry identical charges, creating mutual repulsion that facilitates more uniform distribution across stigmas. As a result, the electrostatic pollination produced kiwifruits with an average weight of 77.41 g, an average horizontal diameter of 49.53 mm, and an average vertical diameter of 59.13 mm, corresponding to increases of 14.77 %, 4.16 %, and 9.40 %, respectively, compared with the non-electrostatic pollination group.

Natural airflow during pollination can cause pollen loss both in transit to the pistil and after deposition. As these charged pollen particles are transported by airflow toward the flower, two major electrostatic interactions occur simultaneously. The first is the attractive Coulomb force between the charged pollen grains and the grounded pistil surface, which drives pollen toward the stigma and ensures firm adhesion upon contact. The second is the mutual repulsive force among the similarly charged pollen grains, which induces slight lateral dispersion during flight and prevents excessive local accumulation. The interaction between these forces establishes a dynamic balance in which attraction ensures target deposition, while repulsion promotes spatial uniformity of pollen coverage on the stigma. Near the pistil tip, the curvature of the stigma enhances local electric field strength, further increasing the electrostatic attraction of pollen particles and facilitating directional deposition. Once pollen grains adhere to the stigma, their residual charge improves attachment stability by resisting detachment caused by airflow disturbances. This coordinated mechanism leads to the formation of a dense and uniformly distributed pollen layer (Oh et al., 2025). As shown in Fig. 10, the variability in kiwifruit size and seed count was lower under electrostatic pollination than non-electrostatic pollination, indicating greater uniformity. Although the overall variation in fruit weight was similar between treatments, the average fruit weight was higher with electrostatic pollination.

Compared with prior kiwifruit pollination techniques, the precision-targeted electrostatic end-effector introduced in this study yields a statistically significant advance in pollination outcomes. Gao et al. (2023) reported that dry pollen outperformed liquid pollen for kiwifruit, increasing fruit set and quality by 9.6 %. Pathak (2025) further observed that either dry or wet pollen delivery improved fruit quality by 10.8 % relative to bee pollination. Gan et al. (2003) attempted wide-area electrostatic spraying and reported a 13.2 % rise in seed number, yet the difference failed to reach statistical significance ($p > 0.05$). In contrast, in this study field experiments demonstrated statistically significant performance enhancements ($p < 0.05$), including an 11.61 % fruit quality improvement over non-electrostatic methods. These findings confirm the technical feasibility and superiority of electrostatic pollination for optimizing kiwifruit production.

Although minor variations in fruit quality and seed number were observed among replicates, these differences may be attributed to microclimatic fluctuations during field operation, such as changes in humidity and airflow turbulence that influence pollen charge retention and trajectory stability. Nevertheless, the overall consistency of the results demonstrates that the electrostatic-assisted airflow pollination system performs reliably under variable orchard conditions. From a practical standpoint, the developed system offers notable advantages for kiwifruit growers. By enhancing pollen adhesion and deposition uniformity, it minimizes pollen waste and ensures efficient fertilization even in windy or low-humidity environments. Furthermore, the low-voltage induction charging method greatly reduces energy consumption and safety risks compared with conventional high-voltage sprayers, while the airflow-guided design enables rapid and precise mechanical pollination. Together, these features represent an important step towards sustainable, energy-efficient, and intelligent pollination technology for precision horticulture.

Table 1
Comparison of pollination performance between electrostatic and non-electrostatic treatments.

Parameter	Electrostatic pollination (Mean ± SE)	Non-electrostatic pollination (Mean ± SE)	P-value
Fruit weight (g)	77.41 ± 6.40	67.45 ± 6.25	1.78×10^{-5}
Seed count	692.00 ± 48.36	620.33 ± 77.02	1.66×10^{-2}
Horizontal diameter (mm)	49.53 ± 1.34	47.55 ± 2.96	0.62×10^{-2}
Vertical diameter (mm)	59.13 ± 1.66	54.05 ± 4.02	1.03×10^{-6}
Fruit set rate (%)	96.25	93.75	

4. Conclusions

An electrostatic-assisted airflow pollination end-effector was specifically designed for kiwifruit flowers, aiming to enhance pollination precision and efficiency through the integration of induction charging and airflow-guided pollen transport. The optimized system achieved a fruit set rate of 96.25 % and significantly improved fruit weight, seed count, and size compared with non-electrostatic pollination, confirming that an appropriate charge-to-mass ratio and electrode configuration can effectively enhance pollen adhesion and uniform deposition on the stigma. These findings establish a parameter-optimized framework for electrostatic pollination, providing both theoretical insight and practical validation for mechanized precision pollination in fruit crops. The integration of induction charging with directed airflow not only improves pollen utilization and deposition efficiency but also reduces energy consumption and operational risks. Looking forward, future work will focus on optimizing electrode geometries, validating system adaptability across different crops, and incorporating automated sensing and control modules to enable intelligent, real-time electrostatic pollination under varying field conditions.

Declaration of Generative AI and AI-assisted technologies in the writing process

During the preparation of this work the authors used ChatGPT in order to improve the readability and language of the manuscript. After using this tool, the authors reviewed and edited the content as needed and take full responsibility for the content of the published article.

CRediT authorship contribution statement

Yusong Ding: Writing – original draft, Methodology, Investigation, Data curation. **Leilei He:** Writing – original draft, Methodology, Investigation, Data curation. **Juncai Huang:** Writing – review & editing, Methodology, Conceptualization. **Xin Wei:** Writing – review & editing, Methodology. **Yufei Shi:** Writing – review & editing, Methodology, Conceptualization. **Hin Lim:** Writing – review & editing, Methodology, Conceptualization. **Spyros Fountas:** Writing – review & editing, Methodology, Conceptualization. **Shaojin Wang:** Writing – review &

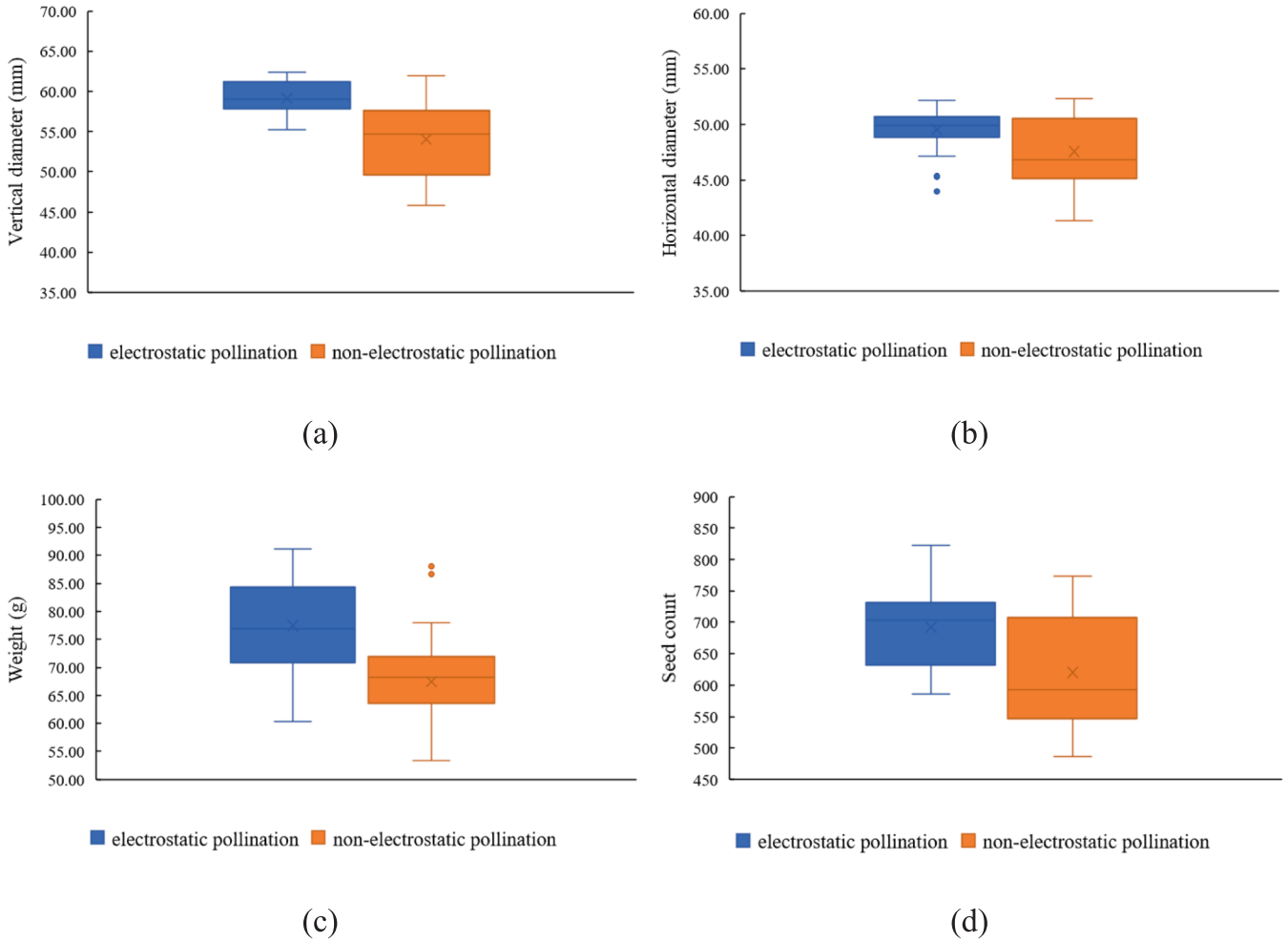


Fig. 10. Boxplot of kiwifruit quality statistics for horizontal diameter (a), vertical diameter (b), weight (c), and seed count (d) between electrostatic and non-electrostatic pollination.

editing, Methodology, Conceptualization. **Rui Li:** Writing – review & editing, Methodology, Conceptualization. **Longsheng Fu:** Writing – review & editing, Supervision, Methodology, Conceptualization.

Declaration of competing interest

The authors declare that they have no known competing financial interests or personal relationships that could have appeared to influence the work reported in this paper.

Acknowledgements

This work was partially supported by National Natural Science Foundation of China (32371999); Key Research and Development Program of Shaanxi (2024PT-ZCK-27, 2024NC-YBXM-195); Jiangxi Provincial Key Laboratory of Modern Agricultural Equipment (Grant Number 20242BCC32127); Science and Technology Program of Xi'an City, China (23NYGG0071); National Foreign Expert Project, Ministry of Human Resources and Social Security, China (H20240238, Y20240046).

Data availability

Data will be made available on request.

References

Abbate, A.P., Campbell, J.W., Williams, G.R., 2023. Artificial pollination of kiwifruit (Actinidia chinensis Planch. var. chinensis) (Ericales: Actinidiaceae) results in greater fruit set compared to flowers pollinated by managed bees (Apis mellifera L. (Hymenoptera: Apidae) and Bombus impatiens Cresson (Hymenoptera: Apidae)). J. Econ. Entomol. 116, 674–685. https://doi.org/10.1093/jee/toad044.

Bechar, A., Gan-Mor, S., Ronen, B., 2008. A method for increasing the electrostatic deposition of pollen and powder. J. Electrostat. 66, 375–380. https://doi.org/10.1016/j.elstat.2008.03.007.

Bechar, A., Shmulevich, I., Eisikowitch, D., 1999. Modeling and experiment analysis of electrostatic date pollination. Trans. ASAE 42 (6), 1511–1516. https://doi.org/10.13031/2013.13314.

Broussard, M.A., Goodwin, M., McBrydie, H.M., Evans, L.J., Pattemore, D.E., 2021. Pollination requirements of kiwifruit (Actinidia chinensis Planch.) differ between cultivars 'Hayward' and 'Zesy002'. New Zeal. J. Crop Hortic. Sci. 49 (1), 30–40. https://doi.org/10.1080/01140671.2020.1861032.

Castro, H., Siopa, C., Casais, V., Castro, M., Loureiro, J., Gaspar, H., Castro, S., 2021. Pollination as a key management tool in crop production: Kiwifruit orchards as a study case. Sci. Hortic. 290, 110533. https://doi.org/10.1016/j.scienta.2021.110533.

Clarke, D., Morley, E., Robert, D., 2017. The bee, the flower, and the electric field: electric ecology and aerial electroreception. J. Comp. Physiol. a Neuroethol. Sensory, Neural. Behav. Physiol. 203, 737–748. https://doi.org/10.1007/s00359-017-1176-6.

Gan-Mor, S., Bechar, A., Ronen, B., Eisikowitch, D., Vaknin, Y., 2003. Electrostatic pollen applicator development and tests for almond, kiwi, date, and pistachio-an overview. Sustain. 11, 1–14. https://doi.org/10.13031/2013.13099.

Gao, C., He, L., Ding, Y., Murengami, B.G., Chen, J., Zhou, C., Ye, H., Li, R., Fu, L., 2025. A novel multinozzle targeting pollination robot for clustered kiwifruit flowers based on air–liquid dual-flow spraying. J. F. Robot. 42 (5), 2136–2150. https://doi.org/10.1002/rob.22499.

Gao, C., He, L., Fang, W., Wu, Z., Jiang, H., Li, R., Fu, L., 2023. A novel pollination robot for kiwifruit flower based on preferential flowers selection and precisely target.

Comput. Electron. Agric. 207, 107762. https://doi.org/10.1016/j.compag.2023.107762.
Gudowska, A., Cwajna, A., Marjańska, E., Moroń, D., 2024. Pollinators enhance the production of a superior strawberry – a global review and meta-analysis. Agric. Ecosyst. Environ. 362, 108815. https://doi.org/10.1016/j.agee.2023.108815.
Han, H., Wang, H., Zhang, Q., Yang, T., Li, X., Zhang, C., Terbish, N., 2024. Experimental study on the charge characteristics and dust reduction performance of inductive electrostatic dual-fluid nozzle for dust pollution control. Powder Technol. 434, 119343. https://doi.org/10.1016/j.powtec.2023.119343.
Hao, W., Wang, X., Zhang, J., Li, R., Fu, M., 2025. Design and experiment of pollination wind tunnels: a novel approach for studying artificial pollination in kiwifruits. Comput. Electron. Agric. 237, 110644. https://doi.org/10.1016/j.compag.2025.110644.
He, L., Liu, X., Ding, Y., Jing, X., Dang, H., Gilbert, B., Janneh, L.L., Li, R., Fountas, S., Garcia, J., Barbedo, A., Fu, L., 2025. Advancements in artificial pollination of crops: from manual to autonomous. Comput. Electron. Agric. 231, 110067. https://doi.org/10.1016/j.compag.2025.110067.
Khatawkar, D.S., James, S.P., Dhalin, D., 2021. Role of electrostatics in artificial pollination and future agriculture. Curr. Sci. 120, 484–491. https://doi.org/10.18520/cs/v120/i3/484-491.
Li, G., Fu, L., Gao, C., Fang, W., Zhao, G., Shi, F., Dhupia, J., Zhao, K., Li, R., Cui, Y., 2022a. Multi-class detection of kiwifruit flower and its distribution identification in orchard based on YOLOv5l and Euclidean distance. Comput. Electron. Agric. 201, 107342. https://doi.org/10.1016/j.compag.2022.107342.
Li, G., Suo, R., Zhao, G., Gao, C., Fu, L., Shi, F., Dhupia, J., Li, R., Cui, Y., 2022b. Real-time detection of kiwifruit flower and bud simultaneously in orchard using YOLOv4 for robotic pollination. Comput. Electron. Agric. 193, 106641. https://doi.org/10.1016/j.compag.2021.106641.
Mamidi, V.R., Ghanshyam, C., Kumar, P.M., Manoj-Kumar, P., 2013. Electrostatic hand pressure knapsack spray system with enhanced performance for small scale farms. J. Electrostat. 71 (4), 785–790. https://doi.org/10.1016/j.elstat.2013.01.011.
Mohanty, S.P., Raheman, H., 2024. Performance optimization of an air-assisted electrostatic spraying unit using response surface methodology. J. Electrostat. 131, 103963. https://doi.org/10.1016/j.elstat.2024.103963.
Nakao, Y., Haruki, T., Murase, K., Morita, Y., Morita, T., 2025. Effects of pollination of some stigmas in kiwifruit flowers on seed distribution and fruit quality. Hortic. J. 94, 184–189. https://doi.org/10.2503/hortj.SZD-009.
Oh, Y.H., Jo, S.H., Son, J., Jeong, H.B., Seo, S.H., Kim, T.H., Son, Y.S., 2025. Innovative electrostatic spray technology for control of particulate matter emitted from electron beam flue gas treatment process. Process Saf. Environ. Prot. 196, 106932. https://doi.org/10.1016/j.psep.2025.106932.
Ou, M., Dai, S., Jing, X., Jia, W., Dong, X., Wang, Y., Wu, M., 2025. Study on spray deposition effect of a new high-clearance air-assisted electrostatic sprayer. Agric. 15 (13), 1331. https://doi.org/10.3390/agriculture15131331.
Patel, M.K., Praveen, B., Sahoo, H.K., Patel, B., Kumar, A., Singh, M., Nayak, M.K., Rajan, P., 2017. An advance air-induced air-assisted electrostatic nozzle with enhanced performance. Comput. Electron. Agric. 135, 280–288. https://doi.org/10.1016/j.compag.2017.02.010.
Pathak, H.S., 2025. Effect of wet or dry pollen application methods on 'Hayward' kiwifruit production. New Zeal. J. Crop Hortic. Sci. 53, 285–297. https://doi.org/10.1080/01140671.2022.2157447.
Siviter, H., Bailes, E.J., Martin, C.D., Oliver, T.R., Koricheva, J., Leadbeater, E., Brown, M.J.F., 2021. Agrochemicals interact synergistically to increase bee mortality. Nature 596, 389–392. https://doi.org/10.1038/s41586-021-03787-7.
Sun, J., Wang, D., Xiao, X., Yu, Q., Xu, X., Liu, Y., Liu, Z., Shi, F., 2025. Study of pollen deposition performance of an airflow-assisted targeted pollinating device for kiwi fruit flower. Biosyst. Eng. 251, 31–47. https://doi.org/10.1016/j.biosystemseng.2025.01.010.
Tacconi, G., Michelotti, V., Cacioppo, O., Vittone, G., 2016. Kiwifruit pollination: the interaction between pollen quality, pollination systems and flowering stage. J. Berry Res. 6, 417–426. https://doi.org/10.3233/JBR-160138.
Vaknin, Y., Gan-mor, S., Bechar, A., Ronen, B., Eisikowitch, D., 2001. Are flowers morphologically adapted to take advantage of electrostatic forces in pollination? New Phytol. 152, 301–306. https://doi.org/10.1046/j.0028-646X.2001.00263.x.
Vaknin, Y., Gan-Mor, S., Bechar, A., Ronen, B., Eisikowitch, D., 2000. The role of electrostatic forces in pollination. In: Dafni, A., Hesse, M., Pacini, E. (Eds.), Pollen and Pollination. Plant Systematics and Evolution – Supplementa, vol. 222. Springer, Vienna, pp. 133–142. https://doi.org/10.1007/BF00984099.
Wu, S., Liu, J., Lei, X., Zhao, S., Lu, J., Jiang, Y., Xie, B., Wang, M., 2022. Research progress on efficient pollination technology of crops. Agronomy 12, 2872. https://doi.org/10.3390/agronomy12112872.
Zhang, Y., Huang, X., Lan, Y., Wang, L., Lu, X., Yan, K., Deng, J., Zeng, W., 2021. Development and prospect of UAV-based aerial electrostatic spray technology in China. Appl. Sci. 11 (9), 4071. https://doi.org/10.3390/app11094071.
Zhao, S., Castle, G.S.P., Adamiak, K., 2008. Factors affecting deposition in electrostatic pesticide spraying. J. Electrostat. 66 (11–12), 594–601. https://doi.org/10.1016/j.elstat.2008.06.009.